Shallow marine to fluvial transition in the Siwalik succession of the Kameng River section, Arunachal Himalaya and its implication for foreland basin evolution

Suchana Taral, Tapan Chakraborty, Pascale Huyghe, Peter van Der Beek, Natalie Vögeli, Guillaume Dupont-Nivet

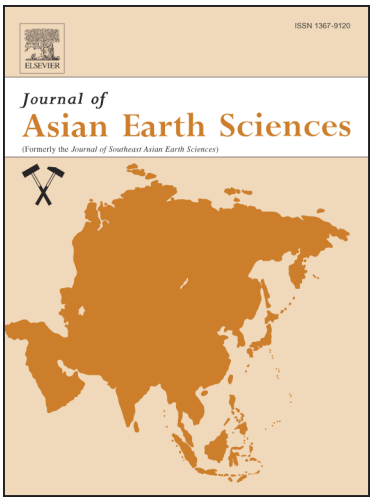

Shallow marine to fluvial transition in the Siwalik succession of the Kameng River section, Arunachal Himalaya and its implication for foreland basin evolution

Suchana Taral, Tapan Chakraborty, Pascale Huyghe, Peter van der Beek, Natalie Vögeli, Guillaume Dupont-Nivet

PII: S1367-9120(19)30332-3
DOI: https://doi.org/10.1016/j.jseaes.2019.103980
Reference: JAES 103980

To appear in: *Journal of Asian Earth Sciences*

Received Date: 21 January 2019
Revised Date: 2 August 2019
Accepted Date: 21 August 2019

Please cite this article as: Taral, S., Chakraborty, T., Huyghe, P., van der Beek, P., Vögeli, N., Dupont-Nivet, G., Shallow marine to fluvial transition in the Siwalik succession of the Kameng River section, Arunachal Himalaya and its implication for foreland basin evolution, *Journal of Asian Earth Sciences* (2019), doi: https://doi.org/10.1016/j.jseaes.2019.103980

Shallow marine to fluvial transition in the Siwalik succession of the Kameng River section, Arunachal Himalaya and its implication for foreland basin evolution

Suchana Taral[1], Tapan Chakraborty[*1], Pascale Huyghe[2], Peter van der Beek[2], Natalie Vögeli[2], Guillaume Dupont-Nivet[3,4]

[1]Geological Studies Unit, Indian Statistical Institute, Kolkata 700108, India

[2]Institut des Sciences de la Terre (ISTerre), Université Grenoble Alpes/CNRS, CS40700, 38058 Grenoble Cedex 9, France

[3]Géosciences Rennes, CNRS/Université Rennes I, CS 74205, 35042 Rennes Cedex, France

[4]Department of Earth and Environmental Sciences, Potsdam University, Germany

*Corresponding author (Chakraborty.tapan@gmail.com)

Abstract

An understanding of the depositional environment and paleogeography of the Siwalik foreland basin are crucial in interpreting the basin configuration, sediment transport pathways and its evolutionary history. This study examines the sedimentology of the Siwalik succession of the Kameng River valley, Arunachal Himalaya, northeastern India. The facies characteristics of the fine-grained, well-sorted sediments of the Dafla Formation and its complex, polymodal paleocurrent pattern in this section, reveals deposition in a variety of open marine to deltaic environment. The overlying Subansiri Formation, characterized by coarse-grained, thick, multistoried sandstone, and showing more consistent SW-ward paleocurrent, indicate deposition from a large, axial braided river system. The proposed redefinition of the boundary between the

Lower Siwalik Dafla and the Middle Siwalik Subansiri formations implies their transition at around 7.5 Ma, instead of 10.5 Ma, suggested earlier. The revised age of the transition is consistent with the age of arrival of the Transhimalayan sediments at 7 Ma and also denotes the time of marine to fluvial transition in this area. Presence of marine sediments in the Kameng section, with similar records further west, indicates the existence of an extensive seaway in the eastern Himalaya during the lower Siwalik time. The extant paleodrainage reconstructions have been recast on the basis of new data on the sedimentology and paleocurrent from this section. It is inferred that the changing sea level, uplifting Shillong Plateau and drainage evolution in the eastern Himalayan foreland during the middle Miocene time controlled the marine to fluvial transition in the basin.

Keywords: Siwalik Group, Kameng River Section, Eastern Himalaya, Sedimentary Facies, Shallow Marine Deposits, Paleocurrent, Basin Analysis

1. Introduction

Sedimentology and paleogeographic analysis are critical for understanding the evolution of sedimentary basins with time (Miall, 2000; Leeder, 2011). The basin-scale geography and mosaic of varied landscape and the depositional processes in a basin are forced by continuous interaction of tectonics and climate (Burbank and Pinter, 1999; Allen, 2008; Clevis et al., 2004). Conversely, careful analysis of basin-fill strata should reveal these tectonic-climatic controls and evolving landscape scenario in a basin (Burbank et al., 1988, Fraser and DeCelles, 1992; Zaleha, 1997; Horton et al., 2004; Huyghe et al. 2005; Rohais et al., 2012). Systematic facies analysis is the main tool for inferring depositional environment and provides a genetic link between stratigraphic architecture and paleogeography in a basin (Miall, 2000).

A number of recent studies in the Siwalik succession of the eastern Himalaya have focused on their depositional age and sedimentary provenance, particularly the arrival of the Transhimalayan detritus and its implication for the evolution of the drainage system (Cina et al. 2009; Chirouze et al., 2012, 2013; Lang and Huttington, 2014; Lang et al., 2016, Govin et al., 2018). However, these studies did not address detailed process-based facies analysis of sedimentary succession to reveal their depositional environment and transport pattern. However, a convincing interpretation of the depositional system and their paleocurrent pattern is a pre-requisite for understanding the pathway of sediment transport from the source to their sink. A detrital sedimentary particle deposited in a shallow marine setting, characterized by a complex flow system, will have a more complex transport pathway that is commonly not related to the regional slope. Whereas a detrital sediment particle transported by a fluvial system moves in a comparatively more linear pathway down the regional slope (Klein, 1967; Tucker, 2001; Clifton, 2006). Recently a variety of wave- and storm-generated structures, trace fossils of marine affinity, and brackish water tolerant spore pollens have been documented from the Siwalik rocks of eastern Himalayan sections of the Tista valley and Bhutan (Taral, 2012; More et al., 2016; Coutand et al., 2016; Taral et al., 2017; Taral and Chakraborty, 2018; Taral et al., 2018). A brackish water influence has also been inferred for the Siwaliks of the Arunachal Himalaya from palynological and botanical studies (Dutta, 1980; Dutta and Singh, 1980; Joshi et al., 2003; Khan et al., 2006). The existing depositional models for the Siwalik succession, as worked out from the Western and Central Himalaya, suggest deposition in an exclusively continental, transversely oriented megafan system (Willis, 1993a, b; Khan et al., 1997; DeCelles et al., 1998; Kumar et al., 1999; Nakayama and Ulak, 1999; Goswami and Deopa, 2015). The new observations from the Eastern Himalaya denote a significant deviation from the

extant depositional models and needs to be taken into consideration while explaining the provenance data, dispersal pattern and stratigraphic evolution of the foreland basin.

This study presents sedimentology of the Siwalik Group exposed along the Kameng River section, a succession which has previously been dated magnetostratigraphically and analyzed for its provenance characteristics, burial/exhumation history, and weathering regime through mineralogical and geochemical analysis (Cina et al., 2009; Chirouze et al., 2012, 2013; Vögeli et al., 2017). One of the main goals of this work is to explore the possible eastward extension of the marine influence that has already been documented from the Tista valley and Bhutan. We propose a minor redefinition of lithostratigraphic boundaries based on the detailed lithologic attributes of the succession. Paleocurrent data collected from different units and have been combined with facies information to understand the sediment dispersal pattern recorded in the succession. Based on the facies analysis and interpreted paleogeography, we show that these sedimentology and paleocurrent data resolves some of the discrepancies between the depositional age and provenance information as suggested by previous works on this succession (Chirouze et al., 2012, 2013). Also, combing the sedimentology with available paleomagnetic and geochemical data from the section allows to develop a well-constrained picture of basin evolution and drainage development in the eastern Himalaya.

2. Geological Background

The Himalayan fold-thrust belt in Arunachal Pradesh can be divided into five major subdivisions. From south to north these are: 1)the Quaternary deposits of the foothills; 2) the Subhimalayan sedimentary succession comprising mainly the Siwalik rocks, 3) the Lesser Himalayan succession consisting of low-grade metamorphic rocks of Proterozoic age (Bomdila Group) and marine

deposits of the Permian Gondwana Group, 4) the Higher Himalayan succession comprising a series of high-grade metamorphic rocks and 5) the Tethyan Himalayan succession comprising Neoproterozoic to Eocene sedimentary rocks that accumulated on the Tethys passive margin of the Indian plate. The major north-dipping faults that separating these tectonostratigraphic units from south to north are Main Frontal Thrust (MFT), Main Boundary Thrust (MBT), Main Central Thrust (MCT), and normal faults of South Tibetan Detachment Zone (STDZ). These tectonostratigraphic units and faults of the eastern Himalayan fold-thrust belt are broadly correlatable with those of the western and central Himalaya (Chirouze et al., 2013; DeCelles et al., 2016 and references therein).

The Kameng River section is located about 115 km east of the Dungsam Chu (Bhutan) and about 400 km east of the Tista valley, the sections from which sedimentology of the Siwalik rocks have previously been reported (Coutand et al., 2016; Taral and Chakraborty, 2018). The Kameng River, oriented broadly Northwest-Southeast in the study area, exposes the Siwalik strata along its course north of the Bhalukpong town (Fig. 1). The Tipi thrust passes through the succession (Yin et al., 2010) and places a thick unit of the Lower Siwalik rocks over the Upper Siwaliks. The Bhalukpong Thrust, to the south of the exposure belt, places the Siwalik rocks over the Quaternary alluvium (Kumar, 1997; Burgess et al., 2012). To the north, the Permian Gondwana succession overthrusts the Siwaliks along the Main Boundary Thrust (Kumar, 1997; Fig. 1).

The Siwalik Group in Arunachal Pradesh is classically divided into the Dafla, Subansiri and Kimin Formations, and have been compared to the Lower, Middle and Upper Siwaliks respectively of the type area in Pakistan (Table 1, Fig. 2; Karunakaran and Ranga Rao, 1976; Chirouze et al., 2012). The Dafla Formation consists of 1-10 m thick, fine- to medium-grained, indurated sandstone alternating with few cm to >2 m thick, grey siltstone and mudstone (Table1, Fig. 3A-C).

Bioturbation and leaf impressions are common. Root traces and large biogenic vertical cylindrical structures of unknown affinity are encountered at places. The Subansiri Formation is characterized by coarse- to very coarse-grained sandstones with common pebbly layers. The sandstone bodies of the Subansiri Formation are at places more than 16 m thick. They are internally characterized by cosets of large planar and trough cross-beds. In the uppermost part of the Subansiri Formation, a few decimeters to meter thick mudstone beds alternate with sandstone beds of comparable thickness (Fig. 2, 3D). The Upper Siwalik Kimin Formation consists of cobble-pebble conglomerate beds that regularly interlayer with fine- to coarse-grained sandstone and dark grey mudstone. Conglomerate beds are 0.5 to 5.0 m thick with alternating fine sandstone and mudstone beds that are a few decimeters to a meter thick. Only a thin strip of the Kimin Formation is exposed in the river bank section north of Tipi village, as the bulk of the formation is truncated by the Tipi Thrust (Fig. 1).

Detail sedimentology of the Siwalik rocks in Arunachal Himalaya is rare. However a number of paleobotanical studies on the Siwaliks of Arunachal Pradesh have inferred brackish water influence in the succession specifically in the Upper Siwalik strata (Kumar, 1997; Joshi et al., 2003; Khan et al., 2006), although the stratigraphic level of samples is not clearly specified, resulting in difficulty to infer the nature, period and extent of brackish water influence in different units of the Siwalik Group based on paleo-botanical evidence alone. An arenaceous foraminifer *Trochammina* sp. (Ranga Rao, 1983) has been reported from the Dafla Formation and a solitary record of vertebrate fossil, *Bos* sp. (Singh, 1977) have also been reported from Arunachal Pradesh. It should be noted that the reported fragment of the *Bos* sp. was collected as a loose material and its stratigraphic position is not clear. Further, despite many intensive studies in this area over the last three decades, reports of freshwater vertebrate fossils have remained conspicuously absent in

the Siwalik strata over the entire eastern Himalaya. It is noteworthy that early workers reported that on many counts the Neogene rocks of the eastern Himalaya differ from that of the western Himalaya, and they proposed that these strata have closer affinity with that of the Neogene rocks of the Assam Basin (Karunakaran and Ranga Rao, 1976; Dutta, 1980).

Chirouze et al. (2012) carried out a detailed magnetostratigraphic study of the Siwalik rocks in the Kameng River section and inferred that the depositional age of the succession range between 13 and 2.5 Ma. They dated the transition from the Dafla to the Subansiri at around 10.5 Ma and that from the Subansiri to the Kimin at around 2.6 Ma. Along the Dungsam Chu section in Bhutan, 100 km to the west, about 2000 m of the Siwalik succession was inferred to be deposited between 7 and 1 Ma (Coutand et al., 2016) where the Dafla to the Subansiri transition was recorded at around 6 Ma. 215 km to the east of the Kameng River, in the Siji River section (Likhabali-Garu area), the paleomagnetically determined depositional age of the lower 1700 m of the supposedly Subansiri Formation was estimated to date between 7.6 and 3.5Ma (Lang et al., 2016). However as base and top of the Subansiri Formation is not exposed in this measured section, these dates are less useful.

3. Methodology

This study focuses on the delineation of facies and facies associations in the Dafla and Subansiri formations using the standard techniques (Reading, 1996; Walker and James; 1992; Walker and Posamentier, 2006). The sedimentary structures were used to define processes of sedimentation whereas vertical and lateral relationships of the primary structures, geometry of the lithosomes and paleocurrent patterns was taken into consideration in defining the facies associations. Paleocurrent data, collected from all the accessible outcrops in the study area, were tilt corrected and plotted in circular histograms using standard methods (Potter and Pettijohn, 1977; Chenney, 1983). About two hundred current vectors have been measured from different facies units (Fig. 1). Detailed

sedimentological logs were measured in selective sections and the position of these detailed logs was marked on the map as well as the in generalized litholog of the entire Siwalik succession of this area (Fig. 2). Based on the available maps and observed lithologic character, boundary between the Dafla Formation and Subansiri Formation is redefined and has been shown in the revised map and the litholog (Figs.1, 2). The conglomerates and sandstones of the Kimin Formation could only be studied along a narrow transect of the Kameng River. Preparation of detailed sedimentary logs and systematic delineation of facies in the Kimin Formation was therefore not possible.

4. Stratigraphy of the Siwalik Group

A detailed examination of the lithopackages (Fig. 2) reveals that the boundary between the Dafla and Subansiri formations, that was proposed earlier (Chirouze et al., 2012), needs some revision. Based on the lithologic attributes of the succession and previous literature, the boundary between these two formations should be placed at the first occurrence of thick beds of coarse-grained sandstone and should be accompanied by a rapid decrease in the proportion of siltstone-mudstone up the succession. Initially the contact between the Dafla and the Subansiri was placed at a stratigraphic level of 1200m in the hanging wall block of the Tipi Thrust (see Fig. 8 of Chirouze et al., 2012). However, 300 meters above this stratigraphic level, the thicker sandstone-dominated succession grades into a ~800 m of fine-grained sandstone-siltstone-mudstone unit. This fine-grained sandstone-siltstone-mudstone successions differ markedly with the thickly bedded, coarse to pebbly, large cross-bedded sandstone typical of the Middle Siwalik Subansiri Formation, well-exposed in the footwall block of the Tipi Thrust. The lower 0-350 m of the measured Siwalik succession (exposed near Bhalukpong town area in the footwall block of the Tipi Thrust) is characterized by laminated, grey mudstone alternating with thinner (up to 2m), fine-grained

sandstone (Fig. 4), that is similar to strata exposed in the hanging wall of the Tipi Thrust (cf. Chirouze et al., 2012). The lithologic character of both the units (the 800 m of strata exposed in the uppermost part of the hanging wall, and the lower most 350 m exposed in the footwall of the Tipi Thrust) are very similar to the classical description of the Dafla Formation (Karunakaran and Ranga Rao, 1976; Gupta, 1997) comprising of fine sandstone-mudstone alternation and differ markedly with the large cross-bedded, coarse-grained sandstone of the Subansiri Formation. These two units, therefore, are marked as the Dafla Formation.

Therefore, in this study we have placed the transition from the Dafla Formation to the Subansiri Formation at the 325 m stratigraphic level above the base of exposed succession in the footwall block of the Tipi Thrust, and consider the entire hanging wall block as the Dafla Formation (Fig. 1, 2). This new delineation of the boundary between the Dafla and the Subansiri is congruent to the original lithostratigraphic definition of these two formations in the Arunachal Himalaya as described by Karunakaran and Ranga Rao (1976) and Kumar (1997). This lithostratigraphic redefinition is also more consistent with the classical definition of the Lower and Middle Siwaliks across the foreland basin (Pascoe, 1963; Acharyya, 1976; Parkash et al., 1980; Kumar, 1997; DeCelles et al., 1998). Moreover, this redefinition, when compared with the magnetic age model of Chirouze et al. (2012), would imply the transition of the Dafla to the Subansiri occurred at around 7.5 Ma, rather than at 10.5 Ma, as proposed in the earlier study of this section (Chirouze et al., 2012). This age of transition is closer to the paleomagnetic ages of the same transition (6 Ma) determined from the Dangsam Chu section of Bhutan (Coutand et al., 2016). As discussed in the later part of the manuscript, this revised transition age also resolves some of the inconsistencies between the age of the stratigraphic boundaries, sedimentology and the Nd-Hf isotopic data obtained during earlier work (Chirouze et al., 2013).

5. Sedimentology

Eleven facies, which are recognized from the Siwalik succession exposed along the Kameng River section, are summarized in Table 2. Based on their preferred occurrences in the studied sections, these facies have been grouped into six facies associations (termed FA1 to FA6; Table 3). Each of these associations is inferred to represent a specific depositional sub-environment within the overall paleogeographic setting in which the Siwalik deposition took place in the Kameng area.

5.1. Facies Association 1 (shoreface-offshore transition)

5.1.1. Description: The facies association is mudstone-dominated and is comprised mainly of laminated to bioturbated mudstone beds (Facies F1, F2 in Table 2; Fig. 3A), interlayered with parallel stratified or hummocky cross-stratified sandstone (F8; Fig. 3C) and subordinate wave rippled thin sandstone/siltstone beds (F5). The stacked units of this facies association vary from 1.2 to 4.5 m in thickness. This association locally displays coarsening-upward trends, with increasing proportion of rippled or parallel-stratified sandstone up-section. Bioturbation is intense at places (BI up to 6; Taylor and Goldring, 1993) and the identifiable trace fossils are *Zoophycos* and *Teichichnus* (Fig. 5A, B).

5.1.2. Interpretation: The preponderance of laminated or bioturbated mudstone-siltstone units (F1/F2) together with the presence of *Zoophycos* indicates quite water environment in a lower part of shoreface to off-shore marine setting. The sharp-based, hummocky cross-stratified and wave rippled sandstone/siltstone units encased in *Zoophycos*-bearing mudstone facies, are interpreted as distal storm deposits formed below the zone of fair-weather wave influence (Brenchley et al., 1986; Pullham, 1989; Ainsworth and Crowley, 1994). The coarsening-upward trend of the facies

association reflects progradation of the shoreline (De Raff et al., 1977; Johnson and Baldwin, 1996; Quin, 2008).

5.2. Facies Association2 (deltafront-delta mouth)

5.2.1. Description: This facies association consists of: a) dark grey, laminated mudstone (F1); b) laterally extensive, graded thin siltstones (F3); c) sharp-based, wave-rippled, fine-grained sandstone (F5), and d) less common smaller (10-55 cm thick), lenticular bodies of cross-stratified, fine-grained sandstone (F4) (Fig. 4A, B). Units of this facies association are 2-6 m thick and show a coarsening-up trend. Sparse bioturbation is present with escape traces, mantle and swirl structures and a few, small, *Ophiomorpha* in the siltstone (F3) and fine-grained sandstone beds (Fig. 4B). Comminuted, coalified, vegetal matters are common in this facies association. This facies association is dominant in the upper part of the Dafla Formation exposed near the Bhalukpong town.

5.2.2. Interpretation: The presence of laminated mudstone indicates suspension settlement of clay and the presence of *Ophiomorpha* implies a marine environment for its deposition. Normal, reverse and normal-to-reverse graded thin siltstone layers (F3, Fig. 4B) are identified as hyperpycnite deposits in the delta-front environment and formed from sediment-charged flood outflow at the river mouth (Mulder et al, 2003; Bhattacharya and MacEachern, 2009). The "mantle and swirl" biogenic structures and rare occurrences of mud-lined *Ophiomorpha* indicate formation of soupy ground due to accumulation of fluid mud that suppressed abundance of benthic fauna, a feature typically associated with river-dominated delta-front environments (Buatois and Mángano, 2011). Isolated, thin, sharp-based wave-rippled beds encased in mudstone indicate deposition of distal storm layers in delta-front environment. Lenticular fine-grained, cross-bedded sandstone (F4) with smooth lower boundary at the top of each of the coarsening-upward successions,

represents deposits of distal terminal distributary channels (TDC) that are subaqueous continuation of the on land distributary channels (cf. Olariu and Bhattacharya, 2006). All these features of this association denote a river-dominated distal delta-front depositional environment (Martinsen, 1990; Johnson and Baldwin, 1996; Bhattacharya, 2006; Ahmed et al., 2014; Martini and Sandrelli, 2015). Each of the coarsening-upward units indicates progradation of the individual delta lobes.

5.3. Facies Association 3 (shoreface)

5.3.1. Description: The facies association consists of 4-30 m thick, amalgamated units of well-sorted, very fine- to fine-grained sandstone with rare mud partings. Sandstone units erosively overlie the sandstone-mudstone alternating units of FA1 and are laterally persistent for more than 50 m across the available exposures (Fig. 3A, B). The succession of sandstone beds shows a slightly coarsening and thickening upward trend (Fig. 3A). Usually, hummocky cross-stratified (HCS) and parallel laminated sandstones beds dominate the lower part of the facies association whereas amalgamated beds of swaley cross-strata, plane parallel lamination and low-angle trough cross-strata and ripple lamination (Fig. 6) dominate the upper part of each of the coarsening-upward packages (Fig. 3A, B). Mud beds, occasionally present in the lower part of the facies association, occur as thin partings in the upper part of the succession (Fig. 3A, B).

In addition, in a few sections fine- to very fine-grained sandstone consisting of meter-scale, sigmoidal cross-strata (F9, Fig. 7) and interlayered parallel strata (F8) (well exposed around 2100 m stratigraphic level in hanging wall block of the Tipi thrust, see Fig. 2) occur as an important constituent of the facies association. The foresets of the large-scale cross-beds dip at an angle much less than the angle of repose, have sigmoid shape, merge imperceptibly at the top and bottom of the set with plane parallel laminations (Fig. 7), and display highly variable dip direction, varying from N-NE to S-SW (Fig. 1, location JBH 11). Wave ripple crests measured from underlying FA1

sandstone show a mean NW-SE trend which is at high angle to the primary current lineation found on some of the plane parallel strata of this unit.

Occasionally, *Skolithos*, *Teichichnus* and probable *Glossifungites* (Fig.5) are found from the parallel-stratified fine-grained sandstone (F7). Bioturbation index (BI) is significantly variable and range from 0 to 4. This facies association forms a significant part of the Dafla Formation, exposed north of the Tipi thrust.

5.3.2. Interpretation: Thick, well-sorted, fine- to medium-grained sandstones consisting of parallel strata, low-angle cross-strata and hummocky and swaley cross-strata, are characteristic of shoreface environment (Clifton et al., 1971; Brenchley et al., 1993; Ainsworth and Crowley, 1994; Clifton et al. 2006). The intervening mudstone units of the association represent deposition during low-energy, fair-weather condition. Occurrence of trace fossils like *Teichihcnus* and *Glossifungites* provides additional support for marine interpretation. Upward gradation from HCS-dominated to SCS and low-angle trough cross-strata dominated units, indicates increasing energy conditions as relative position of the depositional site moves up the shoreface. The hummocky and swaley strata indicate periodic storm surges in lower-middle shoreface environment. Low-angle trough cross-stratification is the result of migrating asymmetric combined flow dunes in the shoreface during fair-weather condition (Arnott and Southard, 1990; Dumas et al., 2005; Perillo et al., 2014).

The isolated, meter-scale, sigmoid cross-beds of facies 9 are inferred to records of shoreface-attached bars, the accreting flank of which produced low-angle sigmoid foresets. Variable accretion direction denoted by the foresets of the cross-beds indicates near symmetrical form of the bars that accreted on both of their flanks. The shoreface attached bars forming under tide or storm-wave induced shallow marine current system has been documented by large number of

workers (Swift and Field, 1981; Johnson, 1977; Cotter 1985; van de Meene et al., 1996). However, lack of evidence of tidal flow asymmetry in the Dafla succession favors a deposition through storm-wave processes.

The wave-ripple crests measured from immediately underlying facies associations show NW-SE trends of local shoreline. The north-dipping foresets of F7 and F9 units appear to be formed by onshore current related to velocity asymmetry generated by shoaling waves in a high energy middle-upper shoreface environment (Hunter et. al., 1979). South-dipping foresets in the facies association indicate storm induced offshore directed current (see Clifton et al., 1971; Clifton, 2006). NW-SE ward flow (parallel to shoreline) components measured from FA3 are probable longshore current. Absence of intense bioturbation or local presence of *Skolithos* is consistent with high energy condition of shoreface environment. Presence of *Teichichnus* and *Glossifungites* indicate hard ground in a non-deltaic sandy shallow marine environment in contrast to evidence of soupy ground associated with FA2.

5.4. Facies Association 4 (coastal bars)

5.4.1. Description: This association consists of planar to low-angle laminated fine-grained sandstone (F7, F8) organized in flat-based, convex-upward, mound-shaped sandstone bodies capped by wave ripples (F5) (Fig. 8). The convex-upward sandstone bodies, up to 45 cm thick, are interlayered with 10-20 cm thick mudstone-siltstone beds (F1). At places amalgamated units of convex-up sandstone bodies alternate with rooted siltstone-mudstone beds and drab-colored paleosol deposits (F10). The mudstone and sandstone beds of the facies association contains abundant comminuted plant debris. FA4 is less frequent than the other facies associations recognized in the Dafla Formation.

5.4.2. Interpretation: Parallel or low-angle stratified sandstone bodies with flat base and convex-up top is interpreted as nearshore coastal bar deposits (Hunter et al., 1979; Chaudhuri and Howard, 1985; Brenchley, 1985; Davies and Gibling, 2003; Clifton, 2006). The wave ripples on the upper surface of the sandstone bodies indicate fair weather wave-modification of the bar-tops (Brenchley, 1985; Midtgaard, 1996). Occurrences of gleyed paleosol and root-penetrated mudstone of F10 indicate existence of sub-aerially emergent coastal plain marshlands that existed close to the coastal bars. This facies association is inferred as deposits of uppermost shoreface to coastal plain environment.

5.5. Facies Association 5 (coastal marsh)

5.5.1. Description: This association comprises 0.2 to 1.2 m thick units of laminated to massive, light yellowish to greenish grey (5BG-4/5Y6/4/Gley1-N3, Munsell Colour Book, 2009) mudstone (F10) interlayered with few cm to dm thick layers of current-, wave- or combined-flow rippled fine-grained sandstone and siltstone (F5, F6). The mudstone beds at places, show large root traces as well as complete destratification with development of fractures and a greenish grey color of the mudstone. The interstratified ripple laminated fine sandstone layers have a sharp basal contact. The root-penetrated massive mudstone, at places, is sharply overlain by undisturbed, thinly laminated dark grey mudstone. At places, decimeter to meter thick flat-based, cross stratified fine-grained sandstone beds alternate with the FA5 mudstones (Fig. 3D). The facies association occurs both in the Dafla and Subansiri exposed in the hanging wall as well as footwall of the Tipi Thrust.

5.5.2. Interpretation: Dark grey mudstone with roots indicates deposition in vegetation-covered shallow pools of stagnant water. Destratification, fracturing, greenish grey colour and root traces denote development of gleyed paleosols (Retallack, 1990; Douchafour, 1982). The rippled sandstones denote periodic sand incursion, similar to that of prograding crevasse delta in marshes

(Perez-Arlucia and Smith, 1999). Overall, FA5 is inferred as deposits of coastal swamp or lower delta plain shallow lakes. Dark grey, laminated mudstone that sharply overlies massive greenish grey mudstone, denote periodic rapid flooding of the marshes. The alternating decimeter-thick sandstone beds with remarkably flat base, as in the upper part of the Subansiri Formation (Fig. 3D), denote subaqueous emplacement of distributaries into these coastal marshes from the adjacent channel belts (McKee, 1957; Taral and Chakraborty, 2018).

5.6. Facies Association 6 (braided stream)

5.6.1. Description: The facies association comprises coarse, pebbly sandstone with 0.5-3.2 m thick planar and trough cross-beds (F11) that are irregularly interlayered with 0.2-1.2 m thick current or combined-flow rippled fine sandstone-siltstone (F6) or massive mudstone. Calcareous concretions, 0.15-1.2 m in diameter, and coalified fossil wood fragments are common throughout. The bulk of the sandstone of this association is organized in 5-15 m thick weakly fining-upward units. The amalgamated units of sandstones form up to 16 m thick sandstone bodies. Flat to slightly undulating erosion surfaces of variable dimension, each lined by thin units of mudclast-rich conglomerate and pebbly sandstone are common throughout the sandstones. Cosets of large-scale cross-strata, at places, migrate over surfaces that are inclined at a low-angle to the downcurrent direction (with respect to the major bounding surfaces), and grades upward into coset of smaller (10-20 cm) cross-sets. This facies association is typical of the Subansiri Formation. In the uppermost part of the Subansiri Formation, some of the thick sandstone beds of this facies association show remarkably flat, sharp basal contact with underlying grey mudstone of FA5 (Fig. 3D).

Tilt-corrected paleocurrent data measured from the association show a comparatively low variability and a west to southeast mean paleo-transport direction (Fig. 1). The paleocurrent

measured from the uppermost part of the Subansiri Formation (JBH22, Fig. 1 and 2), are polymodal in nature and show higher dispersion.

5.6.2. Interpretation: The poorly sorted, coarse-grained sandstone succession with a number of conglomerate-lined, internal erosional surfaces of varying dimension, unidirectional current-generated large planar cross-strata, and the paucity of mudstone are indicative of deposition from a large braided stream system (Collinson, 1996; Best et al., 2003; Miall and Jones, 2003). Pebble-marked undulating erosion surfaces are inferred as bases of channels. The variable dimension of erosion surfaces denotes existence of different orders of channels in a braided river (Best and Bristow, 1993). The downdip inclined cosets of cross-beds represent the downcurrent accreting (DA) macroform elements (Haszeldine, 1983; Miall, 1994; Chakraborty, 1999; Best et al., 2003; Almedia et al., 2016). Southwestward mean paleocurrent in most of the exposures of this facies association are sub-parallel to the local trend of orogenic belt (Fig. 1) and suggest axial nature of the fluvial system similar to the modern Brahmaputra River in northeast India.

In the upper part of the Subansiri Formation, increasing thickness of wave-/combined-flow-rippled siltstone, decimeter to meter-scale pebble-free sandstone units with remarkable smooth base overlying the equally thick grey mudstone beds (Fig. 3D) denote their emplacement as subaqueous distributary channels (terminal distributary channels) of the lower delta plain environment (McKee, 1957; Dasgupta, 2005; Olariu and Bhattacharya, 2006; Taral and Chakraborty, 2018) .

6. Discussion

6.1. Depositional environment

Based on the following features, the sediments of the Dafla Formation are attributed to deposition in an open-marine shoreface to coastal plain setting: a) The sandstones are clean, mica-poor, medium- to very fine-grained, well-sorted (as compared to the overlying Subansiri Formation); b)

abundance of wave- and combined flow generated structures (wave ripple, hummocky cross-strata etc.) throughout the Dafla Formation (Figs. 3, 4, 6); c) presence of flat-based, convex-up sandstone bodies with the top surface marked by wave ripples (Fig. 8); d) occurrence of trace fossils of marine affinity like *Zoophycos*, *Teichichnus*, *Glossifungites*, *Ophiomorpha* etc. (Fig. 5); e) polymodal paleocurrent patterns showing significant modes towards the N or NE (Fig. 1), and f) 7-16 m thick coarsening- and thickening-up successions (Fig. 3A, B)

The overlying Subansiri Formation, on the other hand, is characterized by poorly sorted, pebbly, coarse-grained sandstone with multiple, pebble-lined, erosion surfaces of different dimension, downcurrent-dipping cosets of cross-strata, an upward decrease in the scale of the bedforms and grain size in some of the sandstone units. The paleocurrent directions measured from this Formation show less dispersion, compared to that of the Dafla Formation (Fig. 1). All these features indicate deposition of bulk of the Subansiri Formation from a large braided river system. Occurrence of this variant in the upper part of the Subansiri Formation denote increasing influence of the coastal processes.

The Kimin Formation is characterized by pebble-boulder conglomerates interlayered with cross-bedded sandstone and dark grey mudstone. A proximal alluvial fan depositional system was previously inferred for the Kimin Formation (Chirouze et al., 2012). However, thick beds of grey mudstones and fine-grained sandstones are unlikely to be preserved in a gravelly alluvial fan environment (Blair and McPherson, 1994). It should be noted that throughout the Arunachal Himalaya, the Kimin Formation is marked by the significant presence of mudstone-siltstone beds alternating with pebbly conglomerate and sandstone (Kumar, 1997; Chirouze et al., 2012, Lang et al. 2016). It is also noteworthy that several paleobotanical studies from the upper Siwalik Kimin sediments report recovery of *Palmaepollenites*, which is well-known as a brackish-water tolerant

palynomorph commonly found in nearshore environments (Dutta, 1980; Dutta and Singh, 1980; Kumar, 1997, Coutand et al., 2016). Considering the above aspects, we suggest that the mud-silt bearing part of the Kimin Formation probably represents a fan delta/braidplain delta environment similar to the Upper Siwalik units of the Tista valley (Taral and Chakraborty, 2018). This interpretation is consistent with increasing presence of wave-rippled siltstone, mudstone and terminal distributary channel deposits in the uppermost part of the Subansiri Formation. Thus, the upper part of the Siwalik succession in the Kameng section probably denotes another episode of rising sea level.

A majority of the intervals studied in details are located in the hanging-wall block of the Tipi thrust. These studied intervals are dominated by FA1 to FA5, representing a non-deltaic, shallow marine environment that ranged from the offshore-shoreface transition to a foreshore-coastal swamp environment. This finding implies that the marine deposits recognized in the Siwalik successions of the Tista valley and in Bhutan (Taral and Chakraborty, 2018; Coutand et al., 2016), extend further east. Therefore, a significant part of the eastern foreland basin was part of a marine basin during deposition of the Dafla sediments. The paleogeographic scenario visualized is depicted in figure 9.

The uppermost part of the Dafla Formation, exposed in the footwall block of the Tipi thrust near Bhalukpong town (Fig. 1), on the other hand, is inferred to represent sedimentation in a river-dominated marine delta setting (FA2). This deltaic succession is overlain by a ~2.5 km thick succession of braided fluvial deposits of the Subansiri Formation (FA6). The transition from the deltaic deposits to sandy braided fluvial deposits is marked by sandstone-mudstone alternations unit (Fig. 2). However, when compared with the Siwalik deposits of the Tista valley and Bhutan,

the bulk of the middle Siwalik Subansiri Formation of the Kameng section differ lithologically from them and lacks evidence of marine deposition.

6.2. Stratigraphy, sedimentology and the drainage reconstruction in the EHFB

It has already been pointed out that the stratigraphic redefinition, when combined with paleomagnetic age model of Chirouze et al. (2012), indicate the transition from the Dafla to Subansiri at around 7.5 Ma rather than at 10.5 Ma. In the Kameng section, the boundary between the Dafla and Subansiri also correspond to the transition from marine to continental depositional system, and is therefore in conformity with the recommendation of the code of stratigraphic nomenclature for maintaining congruence between lithostratigraphic boundaries and genetic units (North American Code of Stratigraphic Nomenclature, 1983, article 23e).

Paleomagnetically dated Siwalik succession, combined with the detection of Cretaceous-Paleogene (<200 Ma) detrital zircons or whole rock εNd values from different units of the Siwalik Group has been utilized to reconstruct the arrival of the Transhimalayan sediments in different sections. The presence or absence of the Transhimalayan detritus has been utilized to construct the drainage network in the EHFB (Cina et al., 2009; Chirouze et al., 2013; Govin et al., 2018a, b). It has been observed that most of the Mesozoic to early Paleogene zircons were derived from the Gangdese Batholith terrain, lying northwest of the eastern syntaxial zone of the Himalayan mountain belt. The zircon population with an age distribution around a peak of 500 Ma, on the other hand, were mostly derived from the Higher or Tethyan Himalayan terrain (Cina et al., 2009; Lang and Huttington, 2014, Govin et al., 2018b and references therein). In the Kameng River section, the W-SW paleocurrent pattern of the braided alluvial system of the Subansiri Formation, its age of establishment over the marine Dafla depositional system around 7.5 Ma, and the age of first arrival of the Transhimalayan material around 7 Ma (Chirouze et al., 2013), conjointly point

out to the fact that the Transhimalayan detritus was transported from the east by the axial braided system. A similar phenomenon is still prevailing in the modern Brahmaputra River of the Assam Valley that transports young detrital zircons brought from the Tibetan terrain via Yarlung-Siang connection. The Transhimalayan detritus suffers dilution in their proportion as it is transported through the Brahmaputra fluvial system along the axis of the foreland basin and gets intermingled with the Himalaya-derived sediments (Singh and France-Lanord, 2002). The isotopic signature and zircons dates of the samples collected of many of the modern transverse drainage emanating from the Himalaya are conspicuously depleted in the presence of <200 Ma zircons indicating derivation from the Lasha terrain (Cina et al., 2009; Chirouze et al., 2013; Lang and Huttington, 2014).

The existing drainage reconstruction models in the eastern Himalaya are envisaged on the assumption that both the Transhimalayan or Himalayan detritus are fed to the foreland through fluvial depositional systems. The sediments from a particular provenance must have been transported by a fluvial network; however, the final depositional process affecting them may be different. Thus, sediment brought from the adjacent mountain to its foothill by a drainage network can be reworked and transported up, down or along slope by different processes. Eolian system can transport these materials up the slope, longshore marine transport system can carry this detritus many kilometers parallel to the shoreline, and storm or gravity processes can transport these detritus down the slope to its deeper abyssal plain. The facies analysis of the Siwalik succession in the Kameng area indicates that the Dafla Formation was deposited in a marine environment. Reconstruction of a stream network is not meaningful in these marine units although the question of transport pathway is important. Further, the measurement from the Dafla Formation yield a significant number of paleocurrent vectors to the northern quadrant (Fig. 1) that is inconsistent

with their deposition by a south flowing Himalayan stream system. Transport pathway in a shallow marine setting can be very complex owing to superposition of fair-weather wave agitation, tidal current, longshore current and storm-induced geostrophic currents (Klein, 1967; Johnson and Baldwin, 1996; Tucker, 2001; Clifton, 2006). This complexity in transport vectors is probably reflected in the more complex paleocurrent pattern of the Dafla Formation including a significant northward (hinterlandward) component of the paleocurrent data. The sediments derived from the Transhimalayan terrain, even if it reaches the marine shelf or delta-front region, its transport path may be significantly more complex than down the slope of the basin path followed by a fluvial system. In spite of the fact that the Gangdese Batholith derived sediment started coming to the easternmost corner of the foreland basin via Yarlung-Siang pathway from middle to late Miocene time (Lang and Huttington, 2014; Govin et al., 2018b), a marine environment may delay its arrival in a significant proportion to the Kameng section situated more than 300 km away from the Siang-Brahmaputra confluence. At the same time this detritus might have been transported through a different pathway within the marine basin to reach the contemporaneous deposits of the Bengal Basin and Bengal Fan (Uddin and Lundburg, 1998; Galy et al., 2010; Bracciali et al. 2015; Fig. 9A). In summary, absence of the Transhimalayan material need not imply establishment of a south-flowing, Himalaya-fed fluvial depositional system in the basin. It is reasonable to assume that all along the foreland basin the Himalayan detritus were fed into the basin, and was intermingled with detritus from other provenance (the Transhimalayan or other). The absence or dominance of materials of different provenance in a particular stratigraphic level, in one specific section in the Siwalik succession should be a function of transport processes and path dictated by the paleogeography, rather than the establishment of a different fluvial drainage system. This is

probably the reason for absence of the Transhimalayan sediment in the Kameng section prior to 7 Ma or in the Dangsam Chu section in Bhutan prior to 5 Ma.

It is noteworthy in this context that the braided fluvial deposits of the Dungsam Chu section, dated to have been deposited after ~5 Ma (Coutand et al., 2016) show presence of the Transhimalayan detritus whereas the underlying marine-deltaic sediments of the Lower Siwalik and lower part of the Middle Siwalik, lack evidence of the same (Govin et al., 2018a). Therefore, Transhimalayan detritus recognized in the Siji River section from around 13 Ma reached Kameng area around 7 Ma and the Dungsam Chu section around 5 Ma. The combined evidence, therefore, strongly suggest a correlation between the presence of the Transhimalayan detritus and the establishment of an axial braided fluvial system. As the fluvial depositional system propagated gradually westward, younger and younger horizons record the first appearance of Transhimalayan detritus. This also explains the diachroneity of the transition of marine to the fluvial system in the Kameng and Dangsum Chu sections. However, it should be noted that in the Bhutan section, the transition from the Lower to Middle Siwaliks does not coincide with the marine to fluvial transition (Coutand et al., 2016). In fact, lithostratigraphic successions being time transgressive in nature the contact should normally show a diachroneity between two sections 100 km apart.

The marine deposits of the Lower Siwaliks was probably having a different sediment transport system, resulting in the absence of significant proportion of the Transhimalayan detritus in the lower part of the Kameng and Dungsam Chu section (Chirouze et al., 2013; Govin et al., 2018a) whereas the same has been recognized from the Bengal Basin and Bengal Fan deposits. The cartoon diagram of Fig 9 shows the visualized paleogeography that depicts inferred extent of the marine inundation, subsequent retreat of the sea and establishment of axial fluvial system in the Kameng area.

6.3. Controls of marine to fluvial transition in the EHFB

The above discussion on the role of west-flowing axial braided system in transporting the Transhimalayan sediment across the eastern foreland brings forth the question as to why the Dafla sea retreated from the foreland basin making room for progradation of a continental stream system. First of all, globally a period younger than 10.5 Ma, has been marked as the period of sea-level fall and has also been recorded from the Bengal Fan deposits (Cochran, 1990; France-Lanord et al., 1993; Miller et al., 2005; Hansen et al., 2013). This must be one of the major reasons for the retreat of the Dafla sea from the Kameng area after 8 Ma. Secondly, from middle Miocene, as the connection between the paleo-Yarlung and paleo-Brahmaputra was established, a significant volume of sediment from the Yarlung catchment basins of the Tibet drained into the Siwalik foreland basin. Together with the supply from the rapidly eroding eastern Himalaya (Singh and France-Lanord, 2002; Vögeli et al., 2017), this additional sediment load evacuated through the steeply sloping Tsangpo gorge, was fed into the foreland basin (Lang and Hutington, 2014). This cumulative sediment load is likely to transform the foreland basin from an underfilled to an overfilled one, resulting in the change from marine to a subaerial fluvial depositional system in the basin. Thirdly, the available record suggest that the rapid exhumation of the Shillong Plateau was initiated some time about 10-8 Ma ago (Biswas et al., 2007, Clark and Billham, 2008; Coutand et al. 2016). Significant surface uplift of the plateau was, however, initiated much later, probably around 4 to 5 Million years ago (Govin et al., 2018; Rosenkranz et al., 2018), an uplift inferred to be decoupled from the exhumation of the continental crust below the Shillong Plateau. The exhumation must have given rise to subtle topography in the submerged basin floor and must have significantly contributed to reducing the marine accommodation space. A similar conclusion has been drawn by other workers from the analysis of seismic and well data of the Surma Basin, located

south of the Shillong Plateau (Najman et al., 2016) or the rate of sedimentation derived from paleomagnetic dates of the Siwalik rocks of Bhutan (Coutand et al., 2016). Although the plateau was probably still below mean sea level, the uplifting crustal surface must have a tangible role in reducing the marine accommodation, making pathway for the progression of the delta and establishment of the subaerial braided stream system of the Subansiri Formation. We postulate the uplifting Shillong Plateau was one of the major factors in reducing the marine accommodation and onset of the fluvial deposition of the Middle Siwalik succession.

Thus, the exhumation of the Shillong Plateau prior to its surface uplift and input of additional sediment load from the Tibetan drainage basin to the foreland had important ramifications in the evolution of the EHFB. Both these changes were crucial in transforming the foreland basin from its underfilled to overfilled state. As a more and more convergent strain of the colliding Asian and Indian plate was taken up by the major basement-cored structural features (Oldham and Dauki faults) surrounding the Shillong plateau, it decreased the accommodation space created in this part of the foreland basin. Such decreasing accommodation space must be instrumental in the major reorganization of the foreland basin paleogeography, as is reflected in the marine to fluvial transition recorded in the Kameng River section. We contend that this major change in the basinal paleogeography and its underlying control of sea level, geomorphology and tectonics could have been overlooked without a carefully collected sedimentological and paleocurrent data.

7. Conclusions

1. The revised lithostratigraphic definition implies the age of transition of the Lower to the Middle Siwalik at around 7.5 Ma rather than at 10.5 Ma as suggested earlier. This age of transition is consistent with the reported isotopic data from this section and now closer to the age of this transition (6 Ma) determined from the Bhutan Himalaya.

2. The facies analysis in the Kameng River section indicates deposition of the Dafla sediments in an open marine setting; the coarse-grained sandy succession in the Subansiri Formation has been deposited by braided rivers. The topmost gravelly Kimin Formation resembles fan/braidplain delta deposit.

3. The complex polymodal paleocurrent pattern of the Dafla Formation is typical of shallow marine successions, whereas a more consistent SW-directed paleocurrent from the Subansiri Formation denotes axial nature of the Subansiri river system.

4. The transition between the marine Dafla and fluvial Subansiri sediments marks a major reorganization in the foreland basin paleogeography. The age of arrival of the Transhimalayan materials around 7 Ma in the Kameng section (Chirouze et al., 2013), matches well with this revised age of the transition. This age relationship strengthens the correlation between the axial braided system propagating from the east to west and emplacement of the Transhimalayan detritus.

5. The sedimentology of the Siwalik rocks in the study area shows that the absence of the Transhimalayan sediment need not denote establishment of a transverse Himalayan fluvial system. Indeed it is cleared that the sediment mixing and complex flow pattern in the Dafla sea was responsible for the absence of significant proportion of the Transhimalayan detritus in the lower stratigraphic level of the Kameng succession.

6. The transition of marine basin to a continental basin would imply filling up of the marine accommodation space that must have been achieved through a conjoint action of falling global eustatic sea level, tectonically driven exhumation of the Shillong Plateau and geomorphologically controlled input of additional volume of the Transhimalayan sediment.

Acknowledgement

The work is a part of first author's PhD thesis from Calcutta University. This forms a part of a collaborative work by the researchers of ISTerre, France and those from Indian Statistical Institute. We acknowledge both the Institutes for providing facilities for this research. Professor S. N. Sarkar of ISI is deeply acknowledged for his comments on the first draft of the manuscript. The authors gratefully acknowledge the assistance of Sounak Roy during the field work. We are deeply indebted to the unnamed reviewers and journal editors for their significant contribution in improving the manuscript.

References

Acharyya, S.K., 1976. On the nature of the main Boundary Fault in the Darjeeling Sub-Himalaya. Geological Survey of India Miscelleneous Publication 24 (2), 395-406.

Ahmed, S., Bhattacharya, J.P., Garza, D.E., Li, Y., 2014. Facies architecture and stratigraphic evolution of a river-dominated delta front, Turonian Ferron sandstone, Utah, U.S.A. Journal of Sedimentary Research 84, 97-121.

Ainsworth, R.B., Crowley, S.F., 1994. Wave-dominated nearshore sedimentation and 'forced' regression: post-abandonment facies, Great Limestone Cyclothem, Stainmore, UK. Journal of the Geological Society London 151, 681-695.

Allen, P.A., 2008. From landscapes into geological history. Nature 451, 274-276.

Almedia, R.P., Freitas, B.T., Turra, B.B., Figueiredo, F.T. Marconato, A., Janikian, L., 2016. Reconstructing fluvial bar surfaces from compound cross-strata and the interpretation of bar accretion direction in large river deposits. Sedimentology 63, 609-628.

Arnott, R.W., Southard, S.B., 1990. Exploratory flow-duct experiments on combined-flow bed configurations, and some implications for interpreting storm-event stratification. Journal of Sedimentary Petrology 60 (2), 211-219.

Best, J.L., Ashworth, P.J., Bristow, C.S., Roden, J., 2003. Three-dimensional sedimentary architecture of a large, mid-channel sand braid bar, Jamuna River, Bangladesh. Journal of Sedimentary Research 73 (4), 516-530.

Best, J.l. and Bristow, J.S., 1993. Braided Rivers. Geological Society Special Publication 75, The Geological Society, London.

Bhattacharya, J.P., 2006. Deltas. In: Posamentier, H.W., Walker, R.G. (Eds.), Facies Models Revisited. SEPM Special Publication 84, 237-292.

Bhattacharya, J.P., MacEachern, J.A., 2009. Hyperpycnal rivers and prodeltaic shelves in the Cretaceous seaway of North America. Journal of Sedimentary Research 79, 184-209.

Biswas, S., Coutand, I., Grujic, D., Hager, C., Stöckli, D., Grasemann, B., 2007. Exhumation and uplift of the Shillong plateau and its influence onthe eastern Himalayas: New constraints from apatite and zircon (U-Th-[Sm])/He and apatite fission track analyses. Tectonics 26, doi:10.1029/2007TC002125.

Blair, T.C., McPherson, J.G., 1994. Alluvial fans and their natural distinction from rivers based on morphology, hydraulic processes, sedimentary processes, and facies assemblages. Journal of Sedimentary Research 64, 450-489.

Bracciali, L., Najman, Y., Parrish, R.R., Akhter, S.H., Millar, I., 2015.The Brahmaputra tale of tectonics and erosion: Early Miocene river capture in the Eastern Himalaya. Earth and Planetary Science Letters 415, 25-37.

Brenchley P.J, Pickerill R.K., Stromberg, J., 1993. The role of wave reworking on the architecture of storm sandstone facies, Bell Island Group (Lower Ordovician), Eastern New foundland. Sedimentology 40, 359-382.

Brenchley P.J., 1985. Storm-influenced sandstone beds. Modern Geology 9, 369-396.

Brenchley, P.J., Romano, M, Guiterrez Marco, J.C., 1986. Proximal and distal hummocky cross-stratified facies on a wide Ordovician shelf in Iberia. In: Knight R.J., McLeanJ.R. (Eds.), Shelf Sands and Sandstones. Memoir, Canadian Society of Petroleum Geologists 11, 241-256.

Bridge, J.S., Best, J.L., 1988. Flow, sediment transport and bedform dynamics over the transition from dunes to upper-stage plane beds: implications for the formation of planar laminae. Sedimentology 35,153-163.

Buatois, L., Mángano, M.G., 2011. Ichnology: Organism-substrate Interactions in Space and Time. Cambridge University Press.

Burbank, D.W., Pinter, N., 1999. Landscape evolution: the interactions of tectonics and surface processes. Basin Research 11, 1-6.

Burbank, D.W., Beck, R.A., Raynolds, R. G. H., Hobbs, R., Tahirkheli, R. A.K., 1988. Thrusting and gravel progradation in foreland basins: A test of post-thrusting gravel dispersal. Geology 16, 1143-1146.

Burgess, W.P., Yin, A., Dubey, C.S., Shen, Z-K, Kelty, T.K., 2012. Holocene shortening across the Main Frontal Thrust zone in the eastern Himalaya. Earth and Planetary Science Letters 357–358, 152–167.

Chakraborty, C., Bose, P.K., 1990. Internal structures of sand waves in a tide-storm interactive system" Proterozoic Lower Quartzite Formation, India. Sedimentary Geology 67, 133-142.

Chakraborty, T., 1999. Reconstruction of fluvial bars from the Proterozoic Mancheral Quartzite, Pranhita-Godavari Valley, India. IAS Special Publication 28, 451-466.

Chaudhuri, A., Howard, J.D., 1985. Ramgundam sandstone: a Middle Proterozoic shoal-bar sequence. Journal of Sedimentary Petrology 55 (3), 392-397.

Chenney, R.F., 1983. Statistical Methods in Geology. George Allen and Unwin, London.

Chirouze, F., Dupont-Nivet, G., Huyghe, P., van der Beek, P., Chakraborty, T., Bernet, M., Erens, V., 2012. Magnetostratigraphy of the Neogene Siwalik Group in the far eastern Himalaya: Kameng section, Arunachal Pradesh, India. Journal of Asian Earth Sciences 44, 117-135.

Chirouze, F., Huyghe, P., van der Beek, P., Chauvel, C., Chakraborty, T., Dupont-Nivet, G., Bernet, M., 2013. Tectonics, exhumation, and drainage evolution of the eastern Himalaya since Section, Arunachal Pradesh 13 Ma from detrital geochemistry and thermochronology, Kameng River Section, Arunachal Pradesh. Geological Society of America Bulletin 125 (3/4), 523-538.

Cina, S.E., Yin, A., Grove, M., Dubey, C.S., Shukla, D.P., Lovera, O.M., Kelty, T.K., Gehrels, G.E., Foster, D.A., 2009. Gangdese arc detritus within the eastern Himalayan Neogene foreland basin: Implications for the Neogene evolution of the Yalu–Brahmaputra River system. Earth and Planetary Science Letters 285, 150-162.

Clark, M.K., Billham, R., 2008. Miocene rise of the Shillong Plateau and the beginning of the end for the Eastern Himalaya. Earth and Planetary Science Letters 269, 337–351.

Clevis, Q., De Boer, P.L., Nijman, W., 2004. Differentiating the effect of episodic tectonism and eustatic sea-level fluctuations in foreland basins filled by alluvial fans and axial deltaic systems: insights from a three-dimensional stratigraphic forward model. Sedimentology 51, 809-835.

Clifton, H.E., 2006. A re-examination of facies models for clastic shorelines. In: Walker, R.G., Posamentier, H. (eds.), Facies Models Revisited. SEPM Special Publication 84, 293-337.

Clifton, H.E., Hunter, R.E., Phillips, R.L., 1971. Depositional structures and processes in the non-barred high-energy nearshore. Journal of sedimentary Petrology 41 (3), 651-670.

Collinson, J.D. 1996. Alluvial sediments. In: Reading, H.G. (Ed.), Sedimentary Environments: Process, Facies and Stratigraphy. Blackwell, Cambridge, 37-82.

Cochran, J.R., 1990. Himalayan uplift, sea level, and the record of Bengal Fan sedimentation at the ODP Leg 116 Sites. Proceedings of the Ocean Drilling Program, Scientific Results 116, 397-414.

Cotter, E., 1985. Gravel-topped offshore bar sequences in the Lower Carboniferous of southern Ireland. Sedimentology 32, 195-213.

Cotter, E., Graham, J.R., 1991. Coastal plain sedimentation in the late Devonian of southern Ireland; hummocky cross-stratification in fluvial deposits? Sedimentary Geology 72, 201-224.

Coutand, I., Barrier, L., Govin, G., Grujic, D., Hoorn, C., Dupont-Nivet, G., Najman, Y., 2016. Late Miocene-Pleistocene evolution of India-Eurasia convergence partitioning between the Bhutan Himalaya and the Shillong Plateau: New evidences from foreland basin deposits along the Dungsam Chu section, eastern Bhutan. Tectonics, DOI: 10.1002/2016TC004258.

Dasgupta, P., 2005. Facies pattern of the middle Permian Barren Measures Formation, Jharia basin, India: The sedimentary response to basin tectonics. Journal of Earth System Science 114 (3), 287-302.

Davies, S.J., Gibling, M.R., 2003. Sedimentology Architecture of coastal and alluvial deposits in an extensional basin: the Carboniferous Joggins Formation of eastern Canada. Sedimentology 50, 415-439.

de Raff, J.F.M., Boersma, J.R., van Gelder, A., 1977. Wave-generated structures and sequences from a shallow marine succession, Lower Carboniferous, County Cork, Ireland. Sedimentology 24, 451-483.

DeCelles, P.G., Carrapa, B., Gehrels, G.E., Chakraborty, T., Ghosh, P., 2016. Along-Strike Continuity of Structure, Stratigraphy, and Kinematic History in the Himalayan thrust belt: The View from North eastern India: Eastern Himalayan Thrust Belt. Tectonics, DOI: 10.1002/2016TC004298.

DeCelles, P.G., Gehrels, G.E., Quade, J., Ojha, T.P., Kapp, P.A., Upreti, B.N., 1998. Neogene Foreland basin deposits, erosional unroofing, and the kinematic history of the Himalayan fold-thrust belt, western Nepal. Geological Society of America Bulletin 110, 2-21.

Duchaufour, P., 1982. Pedology. Pedogenesis and classification. London: Allen and Unwin, pp. 448.

Dumas, S., Arnott, R.W.C., Southard, J.B., 2005. Experiments on oscillatory-flow and combined-flow bed forms: implications for interpreting parts of the shallow-marine sedimentary record. Journal of Sedimentary Research 75 (3), 501-513.

Dutta, S.K., Singh, H.P., 1980. Palynology of the Siwalik rocks of the Lesser Himalayas, Kameng District. IV I.P.C. Proc. 4th Int. Palynol. Conference, India, 1976.

Dutta, S.K., 1980. Palynostratigraphy of the sedimentary formations of the Arunachal Pradesh - 2. Palynology of the Siwalik equivalent rocks of Kameng District. Geophytology 10, 5-13.

Fielding, C.R., 2006. Upper flow regime sheets, lenses and scour fills: Extending the range of architectural elements for fluvial sediment bodies. Sedimentary Geology 190, 227-240.

Fielding, C.R., Allen, J.P., Alexander, J., Gibling, M.R., 2009. Facies model for fluvial systems in the seasonal tropics and subtropics. Geology 37 (7), 623-626.

France-Lanord, C., Derry, L., Michard, A., 1993. Evolution of the Himalaya since Miocene time: Isotopic and sedimentological evidence from the Bengal Fan, *in* Treloar, P.J., and Searle, M.P., eds., Himalayan Tectonics: Geological Society of London Special Publication 74, 603–622.

Fraser, G.S. and DeCelles, P.G., 1992. Geomorphic controls on sediment accumulation at margins of foreland basins. Basin Research 4, 233-252.

Galy, V., France-Lanord, C., Peucker-Ehrenbrink, B., Huyghe, P., 2010. Sr-Nd-Os evidence for a stable erosion regime in the Himalaya during the past 12 Myr: Earth and Planetary Science Letters 290, 474-480.

Goswami, P.K. and Deopa, T., 2015. Channel morphology, hydrology and geomorphic positioning of a Middle Miocene river system of the Siwalik foreland basin, India. Geological Magazine 152 (1), 12-27.

Govin, G., Najman, Y., Copley, A., Millar, I., van der Beek, P., Huyghe, P., Grujic, D., Davenport, J., 2018a. Timing and mechanism of the rise of the Shillong Plateau in the Himalayan foreland. Geology 46 (3), 279-282.

Govin, G., Najman, Y., Dupont-nivet, G., Millar, I., van der Beek, P., Huyghe, P., O'sullivan, P., Mark, C., Vögeli, N., 2018b.The tectonics and paleo-drainage of the easternmost Himalaya (arunachalpradesh, india) recorded in the Siwalik rocks of the foreland basin.American Journal of Science 318, 764–798.

Hansen, J., Sato, M., Russell, G., Kharecha, P., 2013. Climate sensitivity, sea level and atmospheric carbon dioxide. Philosophical Transactions of the Royal Society, 1-31, http://dx.doi.org/10.1098/rsta.2012.0294.

Harms, J.C., 1969. Hydraulic Significance of Some Sand Ripples. Geological Society of America Bulletin 80(3), 363-396.

Haszeldine, R. S., 1983. Fluvial bars reconstructed from deep straight channel, Upper Carboniferous coalfield of northeast England. Journal of Sedimentary Petrology 53, 1223-1247.

Horton, B.K., Constenius, K.N., DeCelles, P.G., 2004. Tectonic control on coarse-grained foreland basin sequences: An example from the Cordilleran foreland basin, Utah. Geology 32 (7), 637–640.

Hunter, R.E., Clifton, H.E., Phillips, R.L., 1979. Depositional processes, sedimentary structures, and predicated vertical sequences in barred nearshore systems, southern Oregon Coast. Journal of Sedimentary Research 49 (3), 711-726.

Huyghe, P., Mugnier, J.L., Gajurel, A.P., Delcaillau, B., 2005. Tectonic and climatic control of the changes in the sedimentary record of the Karnali River section (Siwaliks of Western Nepal). The Island Arc 14, 311-327.

Jobe, Z.R., Lowe, D.R., Morris, W.R., 2012. Climbing-ripple successions in turbidite systems: depositional environments, sedimentation rates and accumulation times. Sedimentology 59, 867-898.

Johnson, H.D., 1977. Shallow marine sand bar sequences: an example from the late Precambrian of North Norway. Sedimentology 24, 245-270.

Johnson, H.D., Baldwin C.T., 1996. Shallow clastic seas. In: Reading, H.G. (Ed.) Sedimentary environment and facies, Blackwell Publishing, Oxford, 232-282.

Jopling, A.V., Walker, R.G., 1968. Morphology and origin of ripple-drift cross-lamination, with examples from the Pleistocene of Massachusetts. Journal of Sedimentary Petrology 38 (4), 971-984.

Joshi, A., Tewari, R., Mehrotra, R.C., Chakraborty, P. P., De, A., 2003. Plant remains from the Upper Siwalik sediments of West Kameng District, Arunachal Pradesh.Journal Geological Society of India 61, 319-324.

Karunakaran, C., Ranga Rao, A., 1976. Status of exploration for hydrocarbons in the Himalayan region- contributions to stratigraphy and structure. Himalayan Geology Seminar, New Delhi. Geoloical Survey of India, Miscelleneous Publication 41 (V), Sec. III. 1-66.

Khan, I.A., Bridge, J.S., Kappelman, J., Wilson, R., 1997. Evolution of Miocene fluvial environments, eastern Potwar plateau, northern Pakistan. Sedimentology 44, 221-251.

Khan, M. A., Gupta, S., Parua, D. K., De., A., De., B., Bera, S., 2006. Palynoassemblage from the Upper Siwalik sediments of Papumpare district, Arunachal Pradesh with remarks on Paleoenvironment. Journal of Botanical Society Bengal 60 (1), 44-49.

Khan, M.A., Bera, S., 2014. On Some Fabaceous Fruits from the Siwalik Sediments (Middle Miocene-Lower Pleistocene) of Eastern Himalaya. Journal Geological Society of India 83, 165-174.

Knaust, D., Bromley, R.G., 2012. Trace Fossils as Indicators of Sedimentary Environments. Development in Sedimentology 64, Elsevier, pp.960.

Klein, G.D., 1967. Paleocurrent Analysis in Relation to Modern Marine Sediment Dispersal Patterns. AAPG Bulletin 51(3), 366-382.

Kumar, G., 1997. Geology of the Arunachal Pradesh. Geological Society of India, Bangalore.

Kumar, R., Ghosh, S.K., Sangode, S.J., 1999. Evolution of a Neogene fluvial system in a Himalayan foreland basin, India. In: Macfarlane, A., Sorkhabi, R.B., Quade,J. (Eds.), Himalaya and Tibet: Mountain Roots to Mountain Tops: Boulder, Colorado. Geological Society of America Special Paper 328, 239-256.

Lang, K.A., Huntington, K.W., 2014. Antecedence of the Yarlung-Siang-Brahmaputra River, eastern Himalaya. Earth and Planetary Science Letters 397, 145-158.

Lang, K.A., Huntington, K.W., Burmester, R., Housen, B., 2016. Rapid exhumation of the eastern Himalayan syntaxis since the late Miocene. Geological Society of America Bulletin 128 (9-10), 1403-1422.

Leeder, M.R., 2011. Tectonic sedimentology: sediment systems deciphering global to local tectonics. Sedimentology 58, 2-56.

Martini, I., Sandrelli, F. (2015). Facies analysis of a Pliocene river-dominated deltaic succession (Siena Basin, Italy): Implications for the formation and infilling of terminal distributary channels. *Sedimentology*, 62, 234-265.

Martinsen, O. J. (1990). Fluvial, inertia-dominated deltaic deposition in the Namurian (Carboniferous) of Northern England. *Sedimentology*, 37, 1099-1113.

McKee, E.D. (1957). Flume experiments on the production of stratification and cross-stratification. *Journal of Sedimentary Petrology*, 27, 129-134.

Mehrotra, R.C., Awasthi, N. and Dutta, S.K., 1999. Study of the fossil wood from the upper Tertiary sediments (Siwalik) of Arunachal Pradesh, India and its implication in palaeoecological and phytogeographical interpretations. Review of Palaeobotany and Palynology 107, 223-247.

Miall, A. D. and Jones, B. G. (2003). Fluvial architecture of the Hawkesbury Sandstone (Triassic), Near Sydney, Australia. Journal of Sedimentary Research, 73, 531-545.

Miall, A. D., 2000. Principles of Sedimentary Basin Analysis, Springer-Verlag berlin Heidelberg, New York.

Miall, A.D., 1994. Reconstructing fluvial macroform architecture from two-dimensional outcrops: examples from the Castlegate Sandstone, Book Cliffs, Utah. Journal of Sedimentary Research 64 (2), 146-158.

Midtgaard, H. 1996. Inner-shelf to lower shoreface hummocky sandstone bodies with evidence for geostrophic-influenced combined flow, Lower Cretaceous, West Greenland. Journal of Sedimentary Research 66, 343-353.

Miller, K.G., Kominz, M.A., Browning, J.V., Wright, J.D., Mountain, G.S., Katz, M.E., Sugarman, P.J., Cramer, B.S., Christie-Blick, N. and Pekar, S.F., 2005. The Phanerozoic record of global sea-level change. Science 310, 1293-1298.

More, S., Paruya, D.K., Taral, S., Chakraborty, T., Bera, S., 2016. Depositional Environment of Mio-Pliocene Siwalik Sedimentary Strata from the Darjeeling Himalayan Foothills, India: A Palynological Approach. Plos One, 11(3), doi:10.1371/journal.pone.0150168.

Mulder, T., Syvitski, S., Migeon, S., Fauge´ res, J.-C., Savoye, B., 2003. Marine hyperpycnal flows; initiation, behaviour and related deposits, a review: Marine and Petroleum Geology 20, 861-882.

Najman, Y., Bracciali, L., Parrish, R.R., Chisty, E., Copley, A. 2016. Evolving strain partitioning in the Eastern Himalaya: The growth of the Shillong Plateau. Earth and Planetary Science Letters 433, 1-9.

Nakayama, K., Ulak, P.D., 1999. Evolution of fluvial style in the Siwalik Group in the foothills of the Nepal Himalaya. Sedimentary Geology, 125, 205-224.

Olariu, C., Bhattacharya, J.P., 2006. Terminal distributary channels and delta front architecture of river-dominated delta systems. Journal of Sedimentary Research 76, 212-233.

Parkash, B., Sharma, R.P. Roy, A.K., 1980. The Siwalik Group (molasse)- sediments shed by collision of continental plates. Sedimentary Geology 25, 127-159.

Pascoe, E.H., 1963. A manual of the geology of India and Burma, III, 1345-2130, Geological Survey of India, Calcutta.

Perez-Arlucia, M., Smith, N.D., 1999. Depositional patterns following the 1870's avulsion of Saskatchewan River (Cumberland Marshes). Journal of Sedimentary Research 69, 62-73.

Perillo, M.M., Best, J.L., Garcia, M.H., 2014. A new phase diagram for combined-flow bedforms. Journal of Sedimentary Research 84, 301-313.

Potter, P.E., Pettijohn, F.J., 1977. Paleocurrent and basin analysis. 2nd Edition.Springer-Verlag Berlin Heidelberg New York, pp. 465.

Pullham, A.J., 1989. Controls on internal structure and architecture of sandstone bodies within Upper Carboniferous fluvial-dominated deltas, County Clare, western Ireland. Geological Society of London, Special Publications 41, 179-203.

Quin, J.G., 2008. The evolution of a thick shallow marine succession, the South Munster Basin, Ireland. Sedimentology 55, 1053-1082.

Ramos, A., Sopena, A., Perez-Arlucea, M., 1986. Evolution of Buntsandstein Fluvial Sedimentation in the Northwest Iberian Ranges (Central Spain). Journal of Sedimentary Petrology 56 (6), 862-875.

Ranga Rao, A., 1983. Geology and hydrocarbon potential of a part of Assam–Arakan basin and its adjacent areas. Journal Petroleum Asia-November, 127-158.

Reading, H.G., 1996. Sedimentary Environments: Processes, Facies and Stratigraphy, 3rd Edition, Blackwell Publishing.

Retallack. J.G., 1990. Soils of the past-An introduction to paleopedology. Boston, Unwin Hyman, 520.

Rohais et al 2012, Basin Research, 24, 198-212

Rosenkranz, R., Spiegel, C., Schildgen, T., Wittmann, H., 2018. Coupling denudation rate and topography in the rainiest place on Earth: Reconstructing the Shillong Plateau uplift history with in-situ cosmogenic ^{10}Be. Earth and Planetary Science Letters. Earth and Planetary Science Letters 483, 39–51.

Singh, G., 1977. On the discovery of the first vertebrate fossil from the Upper Tertiary of Subansiri District, Arunachal pradesh. Indian Minerals 29 (4), 65-67.

Singh, S., France-Lanord, C., 2002. Tracing the distribution of erosion in the Brahmaputra watershed from isotopic compositions of stream sediments. Earth and Planetary Science Letters 202, 645-662.

Singh, T., Prakash, U., 1980. Leaf impressions from the Siwalik sediments of Arunachal Pradesh, India. Geophytology 10 (1), 104-107.

Srivastava, G., Mehrotra,R.C.,Srikarni, C., 2018. Fossil wood flora from the Siwalik Group of Arunachal Pradesh, India and its climaticand phytogeographic significance. Journal of Earth System Science 127, https://doi.org/10.1007/s12040-017-0903-2.

Swift, D.J.P., Field, M. E., 1981. Evolution of a classic sand ridge field: Maryland sector, North American inner shelf. Sedimentology 28, 461-482.

Taral, S., Chakraborty, T., 2018. Deltaic coastline of the Siwalik (Neogene) foreland basin: evidences from the Gish River section, Darjeeling Himalaya. Geological Journal 53, 203–229, DOI: 10.1002/gj.2886.

Taral, S., Sarkar, S., Chakraborty, T., 2018. An ichnological model for a deltaic depositional system: New insights from the Neogene Siwalik Foreland Basin of Darjeeling-Sikkim Himalaya. Palaeogeography, Palaeoclimatology, Palaeoecology 511, 188–207.

Taral, S., Kar, N., Chakraborty, T., 2017. Wave-generated structures in the Siwalik rocks of Tista valley, eastern Himalaya: implication for regional palaeogeography. Current Science 113 (5), 889-901.

Taylor, A.M., Goldring, R., 1993. Description and analysis of bioturbation and ichnofabric. Geological Society of London 150, 141-148.

Tucker, M.E., 2001. Sedimantary Petrology. Blackwell Science, Oxford.

Uddin, A., Lundberg, N., 1998. Cenozoic history of the Himalayan-Bengal system: Sand composition in the Bengal basin, Bangladesh. GSA Bulletin 110(4), 497–511.

Uddin, A., Lundberg, N., 1999. A paleo-Brahmaputra? Subsurface lithofacies analysis of Miocene deltaic sediments in the Himalayan–Bengal system, Bangladesh. Sedimentary Geology 123, 239-254.

van de Meene, J.W.H., Boersma, J.R., Terwindt, J.H.J., 1996. Sedimentary structures of combined flow deposits from the shoreface-connected ridges along the central Dutch coast. Marine Geology 131, 151-175.

van de Meene, J.W.H., van Rijn, L.C., 2000. The shoreface-connected ridges along the central Dutch coast-part 2: morphological modelling. Continental Shelf Research 20, 2325-2345.

Vögeli, N., Huyghe, P., van der Beek, P., Najman, Y., Garzanti, E., Chauvel, C., 2018. Weathering regime in the Eastern Himalaya since the mid-Miocene: Indications from detrital geochemistry and clay mineralogy of the Kameng River Section, Arunachal Pradesh, India. Basin Research 30(1), 59-74.

Vögeli, N., Najman, Y., van der Beek, P., Huyghe, P., Wynn, P.M., Govin, G., van der Veen, I., Sachse, D., 2017. Lateral variations in vegetation in the Himalaya since the Miocene and implications for climate evolution. Earth and Planetary Science Letters 471, 1–9.

Walker, R.G., James, N.P., 1992. Facies models: response to sea level changes. Geological association of Canada Publications, pp. 409.

Walker, R.G., Plint, A.J., 1992. Wave- and storm-dominated shallow marine deposit. In: Walker, R.G., James, N.P. (Eds.), Facies model. Geological association of Canada Publications, 219-238.

Walker, R.G., Posamentier, H., 2006. Facies Models Revisited. SEPM Special Publication, 84.

Willis, B. 1993a. Ancient river systems in the Himalayan foredeep, Chinji Village area, northern Pakistan. Sedimentary Geology 88, 1-76.

Willis, B. 1993b. Evolution of Miocene fluvial systems in the Himalayan foredeep through a two kilometer-thick succession in northern Pakistan. Sedimentary Geology 88, 77-121.

Yin, A., Dubey, C.S., Kelty, T.K., Webb, A.A.G., Harrison, T.M., Chou, C.Y., Célérier, J., 2010. Geologic correlation of the Himalayan orogen and Indian craton: Part 2. Structural geology, geochronology, and tectonic evolution of the Eastern Himalaya. Geological Society of America Bulletin 122 (3/4), 360-395.

Zaleha, M.J., 1997. Fluvial and lacustrine palaeoenvironments of the Miocene Siwalik Group, Khaur area, northern Pakistan. Sedimentology 44, 349-368.

Figure captions:

Fig. 1: Geological map of the Siwalik succession exposed along the Kameng River, western Arunachal Pradesh showing the formation boundaries and bedding plane orientations. The rose diagrams display tilt-corrected paleocurrent vectors measured from different exposures. One dip-strike plotted in the Quaternary alluvium indicates the bedding-plane orientation of the subcrop exposure of the Siwalik rocks. The index map is shown at the top where a red star marks the study area.

Fig. 2: Litholog of the Siwalik succession exposed along the Kameng River, Arunachal Pradesh (modified after Chirouze et al., 2012). Note revised boundaries defined in this study between the Dafla Formation (lower Siwalik) and Subansiri Formation (middle Siwalik). The stratigraphic position of the exposures where detailed sedimentology was carried out has been marked with red stars. See Fig.1 for map location of the study points.

Fig. 3: (A) The sedimentological log measured from the exposure shown in figure 3B (Log 2 in fig. 2). (B) Field photograph depicting the typical features of the Dafla Formation in the hanging wall block of the Tipi Thrust. Note the coarsening- and thickening-up successions of FA1 and FA3 (constituent facies annotated as F1, F2 etc.); the human figure is 165 cm tall. The exposure covers ~3m to ~32m of log shown in figure 3A. (C) Field photograph of facies 8; amalgamated hummocky cross-stratified, fine-grained sandstone unit. Note low-amplitude, up-arched lamina separated by convex- up erosional surfaces (yellow arrowheads). The F8 sandstone overlies a

bed of laminated mudstone with silt partings; road cutting section, north of location AS17 (Fig. 1 and 2). (D) Field photograph of meter-scale, sheet-like sandstone beds alternating with heterolithic mudstone beds, Subansiri Formation, 2550 m level of the log shown in fig. 2. Note remarkably flat base of the sandstone beds that on closer examinations reveal lack of coarse basal lag layers; thick grey mudstone-siltstone units show abundant wave/combined flow ripples.

Fig. 4: (A) Field Photograph showing a succession comprising F1, F3 and F4, arranged in several vertically stacked C-U lithounits. In the bottommost C-U package, position of the fig. 6(B) is shown as a red box. The succession represents facies association FA2 in the Dafla Formation, exposure north of the JBH6 (Fig.1), left bank of the Kameng River; (B) Field photograph of graded mudstone-siltstone (F3) and wave rippled fine-grained sandstone unit (F5) encased in mudstone. Distinct coarsening- and fining-up trends in F3 silty beds are shown (yellow arrowheads). Escape structure (Es) and mantle and swirl structure (MS) present in the exposure. A very small *Ophiomorpha* (Op) burrow is preserved in the F3. Note smooth, erosive base of a cross-stratified sandstone of facies 4 at the top of the photograph (red arrows).

Fig. 5: Trace fossils in the Siwalik rocks of the Kameng River section. (A) *Zoophycos*, in bioturbated mudstone-siltstone units of facies 2, oblique to bedding plane view; Bioturbation Index: 4 (sensu Taylor and Goldring, 1993); (B) *Teichicnus*, in facies 2, oblique view of a subvertical bed, the pen is lying on bedding plane, where tubular form (yellow arrow) is exposed; view at high angle to bedding plane shows successively stacked, tabular spreiten structures (black arrows). Stratigraphic top of the section is marked by the 3D arrow. The part of the pen is 5 cm long; (C) vertical, cylindrical traces of *Glossifungites* in parallel stratified fine sandstone (F8) of shoreface deposits (FA3); (D) *Skolithos* identified by tubular, vertical, lined

burrows seen in sectional view (yellow arrows) whereas circular, opening is visible on the bedding-plane view (red arrows); parallel stratified fine-grained sandstone (F8).

Fig. 6: Field photograph of low-angle trough cross-stratified sandstone (F7) and plane parallel stratification (F8) that grades vertically into ripple-laminated sandstone (F5; marked by yellow arrow). Note the low dip of the foresets. The length of the pen is 16.6 cm. Dafla Formation near exposure JBH 10A (Fig 1 and 2), Kameng River section.

Fig. 7: Field Photo of meter-scale, sigmoidal cross-beds of facies 9 of the Dafla Formation. The man is 157 cm tall. Road cutting north of JBH11 (see Fig.1 and 2 for location).

Fig. 8: Field photograph of FA4 showing alternation of plano-convex sandstone bodies with laminated siltstone-mudstone layers of FA4. Top of the sandstone bodies are wave-rippled (marked by red arrow and enlarged in the inset). The flat base and convex-up top of the sandstone bodies are marked by dashed lines. Dafla Formation, Kameng River section, exposure JBH11A (Fig.1 and 2).

Fig. 9: Cartoon diagrams illustrating paleogeography of the Dafla and Subansiri Formation in the study area (based on the data presented in this paper and the published data). (a) Reconstruction during the Dafla time at (>7.5 Ma <13.5 Ma). Note the drainage in the Siji River section emanating from Transhimalayan terrain although the Tibetan detritus did not reach the Kameng section till the establishment of the braided fluvial system during Subansiri Time. (b) Reconstruction of the Siwalik in the eastern part of the foreland basin during the Subansiri time (<7.5 Ma >5 Ma). Note the advancing Himalayan thrust front and the position of the future Shillong Plateau. The exhumation of the Plateau has consumed the marine accommodation

space. However, the exhuming plateau is yet to create a surface uplift deflecting the Subansiri Fluvial drainage further north and west.

Table captions

Table 1: Generalised lithostratigraphy of the Siwalik Group in the Kameng River section, Arunachal Himalayan region. (Modified after Karunakaran and Ranga Rao, 1976; Kumar,1997; Chirouze et al, 2012)

Table 2. Summary of the sedimentary facies recognized in the Dafla and Subansiri Formations of the Kameng River section.

Table 3.Facies associations of the Siwalik sediments in the Kameng River section-

Table 1: Generalised lithostratigraphy of the Siwalik Group in the Kameng River section, Arunachal Himalayan region. (Modified after Karunakaran & Ranga Rao, 1976; Kumar,1997; Chirouze et al, 2012)

Age	Generalised Lithostratigraphy	Formation	Descr
U. Pliocene-Pleistocene	Upper Siwalik	Kimin Formation	Pebble-cobble conglomerates interlayered with soft, and dark grey mudstone. Large fragment
U. Miocene-Pliocene	Middle Siwalik	Subansiri Formation	Thick beds of friable, pebbly, medium to very coar texture and calcareous concretions; sandstone un mudstone-siltstone beds. Large trough and pla
Mid Miocene	Lower Siwalik	Dafla Formation	Fine- to medium-grained, indurated, greyish white t coloured siltstone-shale layers; burrow r

Table 2. Summary of the recognized sedimentary facies from the Dafla and Subansiri Formations of the Kameng River section:

Facies	General description	Lithology	Sedimentary structures	Bounding surfaces of beds	Bed thickness	Fossil content	C
F1	Dark grey laminated mudstone	Carbonaceous, greenish grey (5BG-4)/ pale olive (5Y6/4) mudstone (Munsell Rock Colour, 2009)	Laminated mudstone with interlayered mm to cm-scale units of very-fine sandstone and siltstone	Usually both base and top are gradational.	0.2 to 0.85m thick units; laterally traceable over ~60m.	At places sand-filled, large, biogenic cylindrical structures present (max. diameter: 3.7cm; max. length:5.2 cm); leaf compressions and impressions and comminuted plant debris common	T c n s f
F2	Massive bioturbated mudstone-siltstone	Dark grey mudstone and clayey siltstone	Thin silty layers with wavy or parallel strata recognisable at places	Sharp to gradational boundary	0.2 to 1 m thick; laterally traceable for more than 50 m.	Identifiable trace fossils are *Zoophycos*, *Teichichnus*.	C b T 1 p s p v
F3	Thin, graded layers of fine sand-silt-clay grade material	Dominantly siltstone layers encased in dark grey mudstone.	Layers of siltstone show normal, inverse or normal to inverse grading; soft-sediment deformation features and gutter cast locally present	Usually sharp base and gradational to sharp top	Vary in thickness from a few mm to 2.5cm;stacked units up to 15cm; a layer can be traced laterally for>50m	Presence of drifted coalified vegetal matter	C s a s C b
Facies	**General description**	**Lithology**	**Sedimentary structures**	**Bounding surfaces of beds**	**Bed thickness**	**Fossil content**	
F4	Lenticular, cross-bedded sandstone	Fine- to medium-grained sandstone	Cross-strata in sandstone beds are up to 25cm thick; low-angle strata and wave/combined flow ripple lamina near the top of the units.	Smooth erosive base and gradational top; bases lack pronounced erosional relief and lag conglomerate	Units 0.25 to 0.6m thick	Sandstone beds are sparsely bioturbated (BI:0-1). A few *Ophiomorpha* burrows could be identified.	
F5	Wave rippled	Moderately well-sorted, fine-grained	Straight, bifurcating crests in plan and symmetrical profile,	Sharp, slightly erosive base;	Individual set thickness few mm to 2 cm,	Sparsely bioturbated	

	sandstone and siltstone	sandstone and siltstone	internal lamina show draping, over-shooting, chevron up-building etc.	locally bioturbated top.	rippled units are up to 1m thick.	
F6	Current /combined flow ripple laminated sandstone-siltstone	Very fine- to fine-grained sandstone and siltstone	The ripples often climb sub-critically and some of the foresets show prominent sigmoidal shape and low-angle toe region.	Undulating, erosive top and gradational to sharp base.	Individual ripple lamina are 0.5-3.5 cm and beds are up to 55 cm thick, which are traceable laterally for >10m.	At places bioturbated; trace makers unidentifiable due to exposure limitations.

Facies	General description	Lithology	Sedimentary structures	Bounding surfaces of beds	Bed thickness	Fossil content	Other f
F7	Low-angle trough cross-stratified sandstone	Well-sorted, very-fine to medium-grained sandstone	Foresets dip<15^0 and are tangential to lower bounding surfaces.	Sharp base and top; slight fining-upward trend	Facies units are up to 0.85 m thick and individual beds are 20-55 cm thick and can be traced laterally for several tens of meters.	No bioturbation was observed in the facies	Facies u into ripp F6. Pala measure usually s dispersi pattern v and SW
F8	Parallel laminated and hummocky -cross-stratified sandstone	Well-sorted, very fine to fine-grained sandstone	low-angle (<10°), undulating strata with gradual thickening and thinning over the depressions or elevations; strata flattens away from the dome or hollow; subtle undulating internal erosion surfaces separate sets of strata	Lower bounding surface over mudstone is sharp, at places with few mudstone chips; gradationally passes upward into F7, F5	Individual facies units 20-50 cm thick; amalgamated units are few meters thick	Sparse to moderate bioturbation is observed in this facies. Identifiable trace fossils are *Skolithos* and *Glossifungites*	Laterally low-ang strata in plane pl at places present

Facies	General description	Lithology	Sedimentary structures	Bounding surfaces of beds	Bed thickness	Fossil content
F9	Isolated, meter-scale, low-angle sigmoidal cross-bedded sandstone	Well-sorted to moderately well-sorted fine-grained sandstone	Cross-beds are characterised by i)<20^0 dip of the foresets; ii) sigmoidal foreset geometry with low-angle tangential toe; iii) lack of angle-of-repose foresets; iv) lateral gradation of foresets to sub-horizontal flat lamination and v) common association with F8.	Upper and lower part of the foresets transitional to flat beds.	Individual cross-beds 60-120cm thick and in longitudinal section traceable for>100m.	-

foreset

Facies	General description	Lithology	Sedimentary structures	Bounding surfaces of beds	Bed thickness	Fossil content
F10	Root-penetrated massive to laminated mudstone-siltstone and rare fine sandstone	Greenish to yellowish grey mudstone and thin siltstone/ fine-grained sandstone	Mudstones are usually massive and fractured; root traces common; fractures are bed confined, randomly oriented; slicken sides on some of the fractures; colour changes from dark grey to mottled pale yellowish grey (5BG-4/5Y6/4/Gley1-N3) up the section.	Basal surface gradational and upper surface sharp and at places overlain by laminated dark grey mudstone	Thickness up to 60cm, laterally traceable for more than 15 m.	Laminations within siltstone-mudstone are bent downward indicating penetration by larger roots; smaller roots and leaf impressions common
F11	Large cross-bedded, coarse-grained, pebbly sandstone	Poorly sorted, medium- to, coarse-grained sandstone with thin conglomerate layers or pebble pockets.	Few decimeter to meter thick trough and planar cross-beds, with angle- of-repose (>22^0), unidirectional foresets	Undulating basal erosion surfaces of the sandstone bodies marked with intra- and extra-formational pebbles layers up to 20 cm thick; in some sections the basal surface of the sandstone bodies are remarkably flat without any lag pebble layer	Cross-sets are 0.15-3.2 m thick and cosets 1.5 to several meters thick; in some cases set thickness and grain size show slight decrease	Drifted, coalified vegetal matter abundant

Table 3.Facies associations of the Siwalik Group of rocks in the Kameng River section:

Facies Association	Facies	Description	Bed Geometry	Palaeocurrent	Ichnofossil	Depositional environment and process Interpretation
FA1	Dominantly F1, F2 & less common F5/F6 and F8	Laminated mudstone with thin layers of sharp-based, wave-rippled/parallel laminated sandstone; thicker sandstone units show hummocky cross-strata (HCS); mudstones intensely bioturbated	Tabular/ sheet like units; thicker sandstone beds are up to1.7 m thick; laterally traceable for >100 m; cm-scale wave-rippled layers	Wave ripple crests oriented NW-SE	Bioturbation Index (BI) (Taylor & Goldingring, 1993) upto 6, identified traces include *Zoophycos* and *Teichichnus*	Lower shoreface-offshore transitional environment favouring mud deposition and intense bio-churning;sandstone with wave/combined-flow ripples and HCS represent periodic incursion by storms in the lower shoreface-off-shore transitional environment
FA2	Dominantly F1, F3, F4 and less common F5	Thinly laminated mudstone with alternating thin, laterally extensive graded siltstone layers; thin wave-rippled fine sandstone beds, and less common thicker, cross stratified, smooth-bottomed sandstone beds.	Laterally extensive mudstone-siltstone units, sandstones lenticular and up to 34 cm thick; the units of this FA forms 2-6 m thick coarsening upwards units.	-	Small *Ophiomorpha* burrows; at places mantle and swirl and escape structures	River-dominated distal delta front-delta mouth; graded siltstones resulting from river mouth flood outflow (hyperpicnites); wave rippled beds are distal storm deposits and lenticular sandstonesare probable distal terminal distributary channel deposits; presence of *Ophiomorpha* confirm brackish water influences.

FA3	Dominantly F8, F7; common F9; rare F1	Amalgamated, thick, fine- to medium-grained sandstone dominated by plane parallel lamination, hummocky-swaley cross strata and low-angle trough cross strata; HCS common in the lower part of the association whereas SCS/low-angle troughs dominate the upper part; units of this facies association show coarsening- and thickening upward trend; isolated large planar sets with low-angle,sigmoidal foresets common at places	Sharply overlies beds of KFA1; Sheet-like laterally traceable for several tens of meter along available exposures, amalgamated beds 4-30 m thick	Variable mean directions from S-SW to N-NE, high circular variance	Bioturbation rare; at places *Skolithos*, *Teichichnus* and probable *Glossifungites* can be identified	Wave- and storm-influenced sandy shoreface environment, plane beds and HCS form in the lower shoreface and the combined flow dunes and swales reflect decreasing depth of the upper shoreface environment. Increasing grain size and sandstone body thickness trend up the succession reflect progradation of the shoreline
FA 4	Dominantly F8, F7, F5, F10 and less common F1	Flat-based, convex-upward sandstone bodies with low-angle to parallel strata and capped by wave ripples or thin mud partings; rooted	Plano-convex sandstone bodies 25-45 cm thick; can be laterally traced for few 10s of meters, F10 units tabluar	Wave ripple crest NW-SE	Trace fossils not observed, plant impressions and roots are common	Flat-based, convex-up geometry of sandstone is typical of wave reworked bars formed in the coastal region; locally overlying rooted mudstone of F10 indicate upward transition

		mudstone-siltstone units at many places overlie the sandstone units.				to emergent coastal marshes
FA5	Dominantly F1,F2, F10, subordinate F5, F6.	Alternation of dark grey rooted, mudstone with wave to current rippled thin sheet-like fine sandstone beds; remarkably flat base of the over and underlying sandstone beds in the upper part of the Subansiri Formation	Sheet, laterally traceable for >35 m, units of this facies association 1.7-3.6 m thick	-	Bioturbations present; but traces unidentified	Grey mudstone denote stagnant water while root traces denote near emergent condition; deposition in floodplain lakes or coastal marshes with occasional emplacement of sand as crevasse delta or splay
FA6	Dominantly F11, subordinate F6	Large planar and trough cross-bedded coarse-grained sandstone, locally pebbly, interlayered rippled very fine sandstone; calcareous concretions of various size; units with multiple basal erosion surfaces with F-U trend. planar sets at places are organised in down current dipping cosets	Individual F-U sandstone units are 1-5 m thick, amalgamated sandstones up to 15 m thick	Mean directions towards SW-S; mostly show lesser variability compared to that of KFA3	Plant roots and wood fragments common	Coarse, thick sandstone with basal erosion surfaces, fining-upward trend, dowmcurrent dipping cross-sets, paucity of mud indicate deposition from large braided streams; flow direction imply axial nature of the fluvial system.

Highlights

- The transition from the Lower to the Middle Siwalik took place around 7.5 Ma.
- The Lower Siwalik of this area is a shallow marine/deltaic deposit.
- A large marine embayment existed at least till ~7 Ma in the eastern Himalaya.
- The Middle Siwalik of this area is an axial braided fluvial deposit.
- The changing sea level, uplifting Shillong Plateau and additional sediment from the Transhimalayan source controlled this marine to fluvial transition.

Declaration of interests

√

☒ The authors declare that they have no known competing financial interests or personal relationships that could have appeared to influence the work reported in this paper.

☐The authors declare the following financial interests/personal relationships which may be considered as potential competing interests:

(TAPAN CHAKRABORTY)

CORRESPONDING AUTHOR

AUTHOR DECLARATION

We wish to confirm that there are no known conflicts of interest associated with this publication and there has been no significant financial support for this work that could have influenced its outcome.

We confirm that the manuscript has been read and approved by all named authors and that there are no other persons who satisfied the criteria for authorship but are not listed. We further confirm that the order of authors listed in the manuscript has been approved by all of us.

We confirm that we have given due consideration to the protection of intellectual property associated with this work and that there are no impediments to publication, including the timing of publication, with respect to intellectual property. In so doing we confirm that we have followed the regulations of our institutions concerning intellectual property.

We understand that the Corresponding Author is the sole contact for the Editorial process (including Editorial Manager and direct communications with the office). He is responsible for communicating with the other authors about progress, submissions of revisions and final approval of proofs. We confirm that we have provided a current, correct email address (chakraborty.tapan@gmail.com) which is accessible by the Corresponding Author and which has been configured to accept email from journal.

Signed by the corresponding author as below:

(Suchana Taral) (Tapan Chakraborty) (Pascale Huyghe) (Peter van der Beek)

(Natalie Vögeli) (Guillaume Dupont-Nivet)